Optics & Laser Technology 151 (2022) 108033

Contents lists available at ScienceDirect

Optics and Laser Technology

journal homepage: www.elsevier.com/locate/optlastec

Full length article

Emission wavelength selection and tuning in the $^4F_{3/2}-{}^4I_{11/2}$ manifolds of a Nd:KGd$(WO_4)_2$ solid-state laser

Miguel Cuenca, Haroldo Maestre *, Adrián J. Torregrosa, Juan Capmany

Department of Communications Engineering-I3E, Miguel Hernández University of Elche, 03202 Elche, Spain

ARTICLE INFO

Keywords:
Solid-state laser
Self-injection locking
External-cavity laser
Tungstate
Laser tuning

ABSTRACT

We present a Nd:KGW laser with a wavelength selectable intracavity loss scheme comprising a notch filter and external-cavity feedback, which enables distinct continuous-wave laser oscillation regimes. Based on the spectroscopy of the $^4F_{3/2}$ - $^4I_{11/2}$ transition in Nd:KGW, we have achieved tunable laser oscillation at either 1067 nm, 1076 nm or 1085 nm corresponding to different spectral peaks of the emission cross-section. An adequate balance of the intracavity loss also allows for dual-wavelength operation at both 1067–1076 nm and 1076–1085 nm peaks, and the inclusion of an additional external reflector permits dual-wavelength oscillation in the vicinity of the main emission peak at 1067 nm. From the external-cavity laser theory perspective, in our approach, the tuning mechanism is treated as an effective intracavity loss instead of an effective reflectivity treatment. The key parameters for further improving the emission wavelength range and tunability are identified and discussed.

1. Introduction

Neodymium-doped Potassium Gadolinium Tungstate crystal (Nd:KGW) is an efficient biaxial laser material with emission in the near-infrared. Due to its anisotropy, absorption and emission occurs in the three main optical indicatrix axes, i.e. N_p, N_g and N_m-axis, depending on the crystal orientation (cut). Absorption and emission cross-sections are stronger for N_m and weaker for Ng polarized fields. The Nd^{3+} ion in KGW can be oscillated at either $^4F_{3/2}$ - $^4I_{9/2}$, $^4F_{3/2}$ - $^4I_{11/2}$ or $^4F_{3/2}$ - $^4I_{13/2}$ transitions. Nd:KGW has a broader absorption and $^4F_{3/2}$ - $^4I_{11/2}$ transition gain spectra if compared to widespread Nd^{3+}-doped laser crystals such as Nd:YAG and Nd:YVO_4. A broader absorption requires less stringent conditions for pump wavelength stability and bandwidth, and a broader emission potentially allows for tunability of the emission wavelength. In addition, KGW (KGd$(WO_4)_2$) host material shows a high nonlinear third-order susceptibility allowing for Raman scattering frequency conversion [1,2]. Nd:KGW lasers are typically diode-laser pumped either around 810 nm, 877 nm or 910 nm, with slope efficiencies up to 70% [3–5]. The main energy levels and transitions for Nd^{3+} in KGW host is shown in Fig. 1(a) [6].

In particular, for an N_p-cut Nd:KGW crystal, which is the crystal orientation of the Nd:KGW in this work, emission from the $^4F_{3/2}$ - $^4I_{11/2}$ transition is strongly polarized parallel to the N_m-direction and peaks at 1067 nm [3,7]. There are additional weaker spectral peaks within the emission cross-section spectrum at 1058, 1076 and 1085 nm (Fig. 1(b)) for which lasing has not been reported yet. Additionally, simultaneous oscillation of these lines has neither been reported so far. In this work we have achieved laser oscillation at either 1067 nm, 1076 nm or 1085 nm with a limited tunability and dual-wavelength operation by means of a combination of intracavity filtering and external-cavity feedback.

These results are of application on the generation of new emission lines through self-Raman effect in Nd:KGW for single-wavelength operation. Dual-wavelength operation has also application in terahertz (THz) generation where two optical frequencies with an adequate offset can be mixed together in a photomixer (fast photoconductor or photodiode) [8] or in a nonlinear optical crystal suitable for difference-frequency generation (DFG) to obtain a signal in the THz spectral range [9]. A more recent application of dual-wavelength lasers is the field-of-view enhancement in infrared (IR) upconversion imaging [10,11]. In this novel application a dual-wavelength laser source can be configured to increase the upconverted area of the IR image and would require, typically, a narrower wavelength offset when compared to that of THz generation.

Laser wavelength selection and tuning is typically achieved by means of either intracavity prism angular dispersion [12], etalon [13], birefringent filters [6] or external-cavity techniques [14], in which the intracavity loss, L_c, or cavity mirror transmission T, is made to be wavelength selective. Common to all these techniques, the lasing

* Corresponding author.
E-mail address: hmaestre@umh.es (H. Maestre).

https://doi.org/10.1016/j.optlastec.2022.108033
Received 13 November 2021; Received in revised form 10 February 2022; Accepted 2 March 2022
Available online 18 March 2022

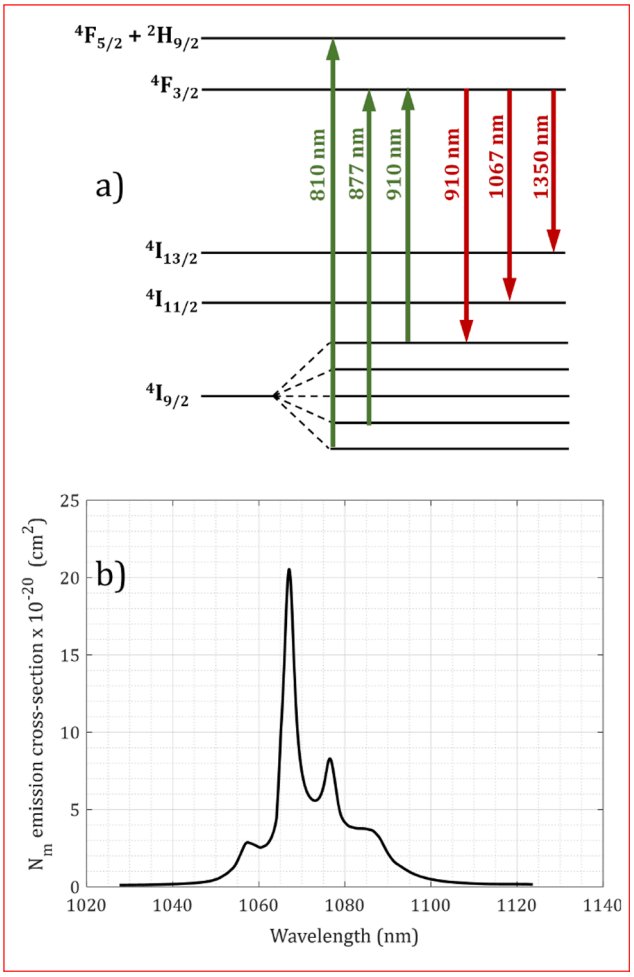

Fig. 1. (a) Energy levels and band diagram [6] and (b) N_m-polarized emission cross-section in Nd:KGW [3,7].

threshold, among other parameters which are relatively wavelength independent, is governed by the ratio of total cavity loss to emission cross-section (Eq. 1) for a given wavelength which, after a slight modification of [14], yields:

$$P_{th}(\lambda) \propto \frac{T(\lambda) + L_c\ (\lambda)}{\sigma_e\ (\lambda)} \tag{1}$$

As it can be drawn from Eq. 1, for a targeted wavelength to oscillate, the laser cavity design must assure that either the intracavity loss or the output coupler transmission, or both, minimize the ratio in Eq. 1 as the emission cross-section is fixed by the laser crystal.

Concerning laser wavelength selection and tuning in Nd-doped hosts, external-cavity tuning has not been fully explored. Typically, in a laser cavity with an intracavity etalon or a birefringent filter, all wavelengths have a very similar transmission in the output mirror and the prevailing wavelength is that for which the intracavity loss of the intracavity element makes Eq. 1 minimum. In contrast, in an external-cavity setup all wavelengths have approximately the same intracavity loss, and the oscillation wavelength is selected by the effective transmission of the combination of output coupler plus an external reflector for which Eq. 1 is also at minimum.

In terms of wavelength selection, when compared to external-cavity tuning, both etalon and birefringent filters have an intrinsic free-spectral-range and, as a result, the periodic transmission peaks may spread to other spectral areas favoring the oscillation of additional wavelengths. In order to modulate the transmission of unwanted peaks, additional etalons or plates, in the case of birefringent filters, need to be

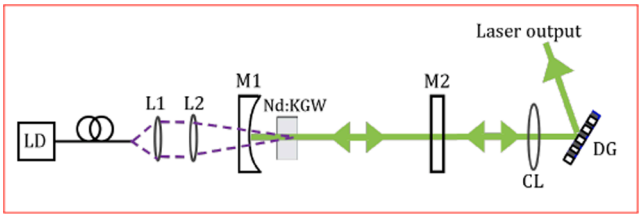

Fig. 2. Experimental setup of the Nd:KGW laser with external-cavity feedback.

added, thus increasing complexity and cost. In this sense, feedback from an external-cavity reflector (i.e. a diffraction grating) focuses only in the neighborhood of the wavelength of interest. In contrast, external-cavity may require a higher number of optical elements than etalon or birefringent filter tuning and, in addition, external-cavity optical elements need to ensure a good mode-matching of the back fed radiation to the fundamental mode of the main laser cavity. Any deviation in mode-matching will reflect a reduction of the amount of feedback effectively coupled to the laser cavity. On the other hand, in the case of etalons and birefringent filter tuning it is necessary to match one spectral resonance of the etalon or the filter to that of one or more cavity axial modes. Likewise, when compared to the external-cavity tuning configuration, an integer relation between the main cavity and the external-cavity lengths is desirable in order to match their axial modes. However, this condition is a much less stringent than that based on etalons or filter tuning since the intracavity loss does not increase if a perfect integer ratio between cavity lengths is not met.

There is also a research interest in tunable intracavity Raman lasers. Tunability of both the laser and the Raman shifted emission has been studied in some Nd-doped hosts. In particular, for Nd:$GdYVO_4$ a 4 nm tuning of the laser line and its corresponding Stokes wavelength was achieved in [13,15]. Such tuning is wider than that achieved in this work but we believe that further investigations on the tuning of the laser line in Nd:KGW can lead to broader tunability due to a wider emission cross-section bandwidth of Nd:KGW when compared to Nd:$GdYVO_4$. The main advantage of external-cavity tuning over etalons and birefringent filters is then in the study of tunability in monolithic solid-state-lasers. Due to the rugged and compact cavity of a monolithic laser [16], no tuning elements such as etalons or birefringent filters can be placed intracavity. In the context of this research, potential monolithic self-Raman Nd:KGW lasers may benefit from external-cavity tuning. Therefore, external-cavity investigations in Nd:KGW are necessary for tuning both laser and Raman conversion in compact monolithic self-Raman Nd:KGW lasers [17].

There is extensive bibliography dealing with wavelength selection in a wide variety Nd-doped materials. As a summary of the most important achievements, the tables in [6,18], and references therein, provide an excellent review on this topic. Thus, we believe our work is a pioneering exploration on wavelength selection and tuning for the first time in Nd:KGW. In this regard, and following the external-cavity theory [14], we expected to achieve oscillation on the 1058, 1076 and 1085 nm laser lines in Nd:KGW, in addition to the widely used 1067 nm emission. Experimental constraints allowed us for only achieving oscillation at 1067, 1076 and 1085 nm. This will be discussed in the following sections.

2. External-cavity tuning in N_p-cut Nd:KGW laser

As a first approach to investigate tuning in Nd:KGW, a two mirror linear cavity with an external-cavity Nd:KGW laser was built (Fig. 2). A diode laser (LD) with peak wavelength emission at 804 nm coupled to a multimode fiber with 105;μm core and 0.22 NA, is used as the laser pump. The output from the multimode fiber is first collimated by the lens L1 an then focused by the lens L2, providing a magnification of nearly 3.5 with a 370 μm pump beam diameter inside the Nd:KGW

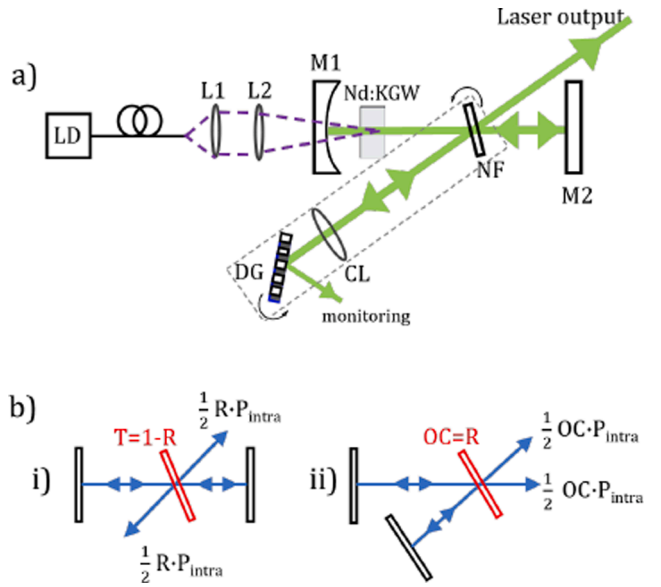

Fig. 3. (a) Experimental setup for wavelength selection and tuning in Nd:KGW. (b) Schematic of the equivalence between i) linear cavity with intracavity filter and (ii) V-shaped cavity configuration.

crystal. Under our available pump power conditions, i.e. a pump intensity <2 kW/cm^2, this spot diameter provides safe CW operation for Nd:KGW, which is prone to crystal fracture [3,19,20]. A plano-concave linear laser cavity is formed between mirrors M1 (concave, roc = 100 mm) and M2 (flat output coupler). Both mirrors are AR coated at the pump wavelength. M1 is HR>99.9% coated and M2 is PR = 96% in the range 1040–1090 nm. The gain material is a 5% doped, N$_p$-cut, 3x3 mm^2 section, 2 mm long Nd:KGW crystal (Optogama UAB), wrapped in indium foil and water cooled down to 15 °C. The absorbed pump power through the crystal was measured to be 65%.

The main cavity length (distance between M1-M2) was 70 mm and the Nd:KGW crystal was separated 15 mm from M1. In this configuration fundamental laser cavity mode had a waist radius of 190 μm, thus providing a good overlap with the pump laser throughout the short crystal length. The external cavity was placed after the output coupler and comprised a collimation lens (CL) with 150 mm focal length and a diffraction grating (DG) in a Littrow configuration. The diffraction grating was a ruled diffraction grating with 1200 lines/mm blazed at 36° for 1 μm. The output of the laser was directed to an optical spectrum analyzer (OSA) with a resolution of 0.06 nm between 1 and 2 μm. We experimentally achieved N$_m$-polarized single-wavelength emission at either 1067 nm (1 nm tuning) and 1076 nm (0.5 nm tuning) and rather unstable dual-wavelength 1067–1076 nm oscillation. When an external-cavity feedback was applied, the oscillation threshold was reduced. The reduction factor is obtained as the ratio of the pump power threshold in free-running oscillation (P$_{th,free}$) to the pump power threshold under external-cavity feedback (P$_{th,eff}$). Under external-cavity feedback, we measured a pump power reduction factor $P_{th,free}/P_{th,eff}$=1.3. The cascade of the output coupler and the external cavity can be viewed as an effective reflectivity (R$_{eff}$) which can be calculated as [14]:

$$R_{eff}(\lambda) = \frac{(r_2(\lambda) + r_{DG}(\lambda))^2}{(1 + r_2(\lambda) r_{DG}(\lambda))^2} \quad (2)$$

where r$_2$ and r$_{DG}$ are the amplitude reflection coefficients of M2 and DG respectively. Ideally r_{DG}^2 provides the fraction of the incoming power which is reflected back from the grating and governs the feedback efficiency. Experimentally, there are several factors affecting the feedback efficiency, thus reducing r_{DG}^2. After analyzing the threshold reduction of 1.3 at 1067 nm we found that under our optical feedback experimental

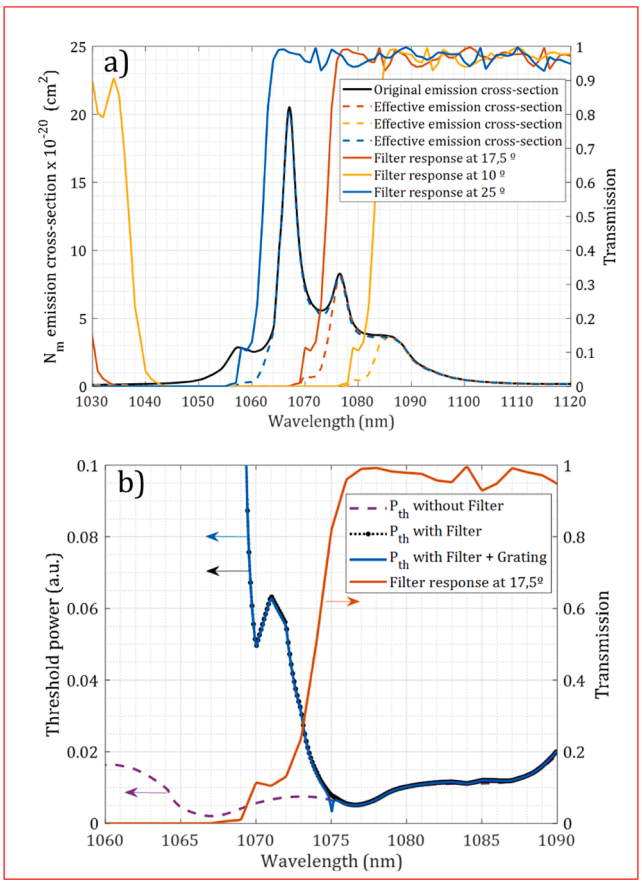

Fig. 4. (a) Angular tuning of the notch filter spectral power transmission and equivalent emission cross-section (dotted lines). (b) Simulation of the power threshold at 1075 nm including NF and external cavity.

conditions, only an effective 25% feedback ratio was achieved, which was not enough to oscillate around 1085 nm, suppressing 1067 and 1076 nm. N$_p$-cut Nd:KGW suffers from astigmatism and opposite sign of the induced thermal focal lens in the N$_g$ and N$_m$-directions [21]. We believe that although a measured 60% of the output power was fed back to the cavity, astigmatism and different sign of the thermal focal lenses in transverse directions made it difficult to mode-match the feedback to the laser mode inside the cavity with a single collimating spherical lens. Besides this, the output beam from M2 was 1.25 mm width on CL and around 1.5 mm width, therefore illuminating 2000 lines in DG and providing a resolution of 0.5 nm. A 0.5 nm width feedback does not effectively couples light to the ~0.1 nm width of the free-running oscillation. Thus, under reduced feedback conditions, an alternative method was needed for selecting and tuning the emission of our Nd:KGW laser since the feedback was not enough to oscillate the targeted wavelengths.

In order to compensate for the low effective feedback, we built a modification of the setup in Fig. 2 by changing M2 reflectivity to HR>99.9% in the range of 1040–1090 nm and including a notch filter. The experimental setup used in our approach for wavelength selection and tuning in a solid-state laser based on Nd:KGW is shown in Fig. 3(a) where NF is an off-the-shelf (commercially available) optical notch filter (Thorlabs NF1064-44) inserted intracavity (33 mm away from M2) to attenuate the strongest emission lines within the $^4F_{3/2}$ - $^4I_{11/2}$ transition, thus allowing the oscillation of lower cross-section wavelengths. The notch filter has a rejection band of 44 nm centered at 1064 nm with 60 dB attenuation and a slope of 4.5 dB/nm on the band edges. Its spectral response can be shifted to shorter wavelengths by means of angle tuning. The passband of the notch filter has a reflectivity of around R = 2–3%,

and acts as a cavity loss which extracts such amount of the intracavity circulating power per trip out of the cavity. In this work this reflection was opportunistically used as an output coupler. As a result, our laser cavity with an intracavity element of transmittance T and reflectivity R = 1-T (Fig. 3(b.i)) can be seen as a V-shaped cavity with a folding mirror of transmittance OC = R (Fig. 3(b.ii)). Therefore, the feedback of the reflected portion of the intracavity power from the NF in our laser resembles a V-shaped cavity configuration under external-cavity feedback and, therefore, external-cavity theory can then be applied for the interpretation of the experimental results.

The output radiation, in addition to a collimating (CL) and a ruled diffraction grating (DG) (dashed square in Fig. 3(a)), can provide an effective spectral shaping of the intracavity loss, thus enabling both wavelength selection and tuning of the emission wavelength. The laser cavity emitted in the N_m polarization and it was aligned perpendicular to the diffraction grating grooves in order to optimize the diffraction efficiency. The combination of the NF loss, reflectivity and external-cavity feedback determines the oscillation wavelength and threshold (Eq. 1). Wavelength selection and tuning is then accomplished by laser threshold compensation, i.e., by increasing the total cavity loss for those wavelengths with higher emission cross-section and, thus obtaining the lowest threshold for a targeted wavelength. Numerical data of angle tuning of the notch filter are plotted in Fig. 4(a). As it can be seen, tuning of the notch filter can be used to cancel the emission-cross section maxima at unwanted wavelengths, yielding a similar cross-section only at long wavelengths within the ${}^4F_{3/2}$ - ${}^4I_{11/2}$ transition. In addition to the action of the filter, we create an effective reduction of the intracavity loss ($L_c \rightarrow L_{c,eff}$) by means of an external cavity rather than an effective increase of the output coupler reflectivity, which is a more spread technique in terms of external-cavity lasers (Eq. 2). The insertion of a notch filter suppresses laser emission of the strongest spectral lines and the band-pass transmission of nearly 98–97% (i.e. R = 2–3%) per single trip can be increased at the targeted wavelength by the optical feedback provided by CL and DG (Fig. 3(a)) in a Littrow configuration. Since M2 (Fig. 3(a)) reflectivity is R2≈100% (T2(λ)→0), wavelength selection and tunability is then only controllable by L_c and Eq. 1 reduces to:

$$P_{th}(\lambda) \propto \frac{L_{c,eff}(\lambda)}{\sigma_e\ (\lambda)} \tag{3}$$

The threshold of the oscillating wavelength is thus governed by the ratio of the effective intracavity loss to cross-section, where $L_{c,eff}=L_{c,0}+T_{eff}$ includes losses of the cold cavity ($L_{c,0}$) and NF transmittance effectively increased by optical feedback ($T_{eff}=1-R_{eff}$).

In Fig. 4(b), we simulate the power threshold for a wavelength of around 1075 nm. The purple dashed line represents the threshold in the absence of NF and external-cavity. The dotted black line is the resulting threshold, including the NF filter response at 17.5° (orange line in Fig. 4 (a) and (b)). The lowest threshold is achieved after the external cavity is inserted (blue line) with a feedback ratio of 25%. The minimum threshold is at the maximum of the grating diffraction efficiency and, as a consequence, it can be tuned as DF is rotated.

3. Experimental results

Since there are two optical outputs in the setup of Fig. 3(a), as in a V-shaped cavity, they can be used to achieve different oscillation regimes if one or more external reflectors are included in the setup [22], depending on the combination of the NF attenuation, i.e. angular position, and optical feedback. We have achieved single-wavelength, short-range tuning and dual-wavelength operation. When configured for single-wavelength operation, the emission was switched at either at 1067 nm, 1076 nm or 1085 nm. For an orientation of 25° of the NF surface to the cavity axis, 1067 nm, 1076 nm or 1085 nm lay in the passband of the filter and emission at 1067 nm, which has the highest cross-section, dominates among the rest. The emission at 1067 nm can be reinforced

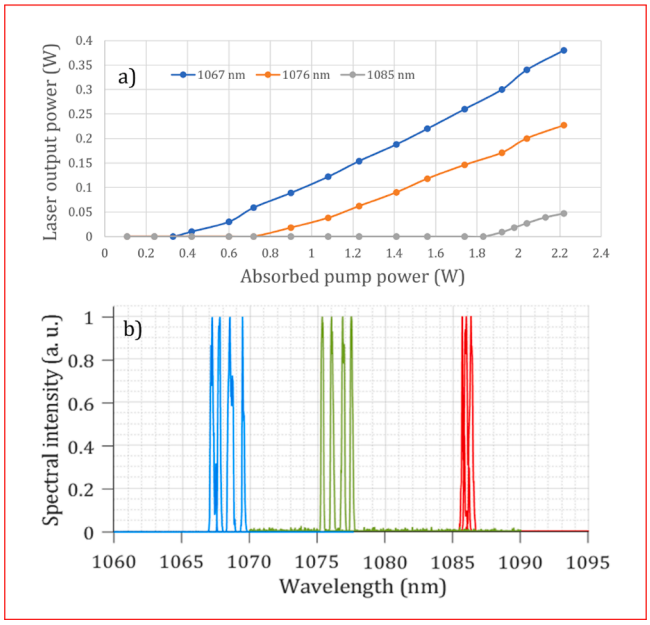

Fig. 5. (a) Laser output power versus pump power for the setup of Fig. 3(a) tuned to either 1067 nm, 1076 nm or 1085 nm. (b) Wavelength tuning in the surrounding of 1067 nm, 1076 nm and 1085 nm.

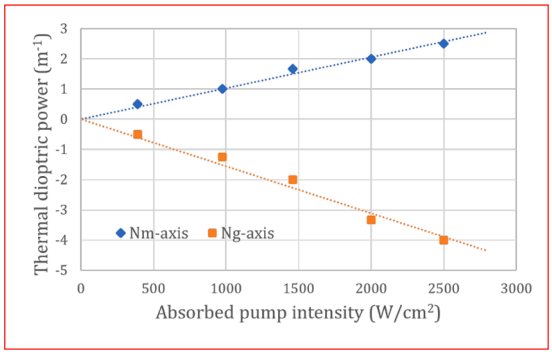

Fig. 6. Thermally induced dioptric power as a function of absorbed pump intensity for N_m and N_g transverse planes.

and its threshold reduced by the inclusion of the external cavity (CL + DF). A slight angle reduction of the NF with regard to the cavity axis places 1067 nm at the stop-band edge with a strong attenuation whereas 1076 nm and 1085 nm are allowed to pass through the filter. Due to a higher emission cross-section in comparison to 1085 nm, oscillation at 1076 nm occurs and can also be reinforced by the grating if properly tuned. A further reduction in the angle between the normal to the filter surface and the cavity axis enhances the loss for 1067 nm and 1076 nm, thus being 1085 nm the wavelength with the highest cross-section in the pass-band of the filter, which can be reinforced by the external cavity as well. In Fig. 5(a) we show the laser output power versus the absorbed pump power for either 1067 nm, 1076 nm or 1085 nm when the combination of NF and DF orientation is the adequate to make only one of them to prevail, i.e. under external-cavity feedback. The pump power reduction factor was also measured for 1067 nm and 1076 nm, which were able to oscillate in the absence of external-cavity feedback. Again, a pump power reduction factor of 1.3 was obtained since thermal lens and feedback spectral resolution are similar to that in experiment in Fig. 2. Besides a threshold reduction, the angular dependence of the diffracted wavelength in the grating enabled a limited tunability of the aforementioned laser lines. Examples of different emission lines and tuning in Nd:KGW are shown in Fig. 5(b). We achieved ~3 nm tuning in

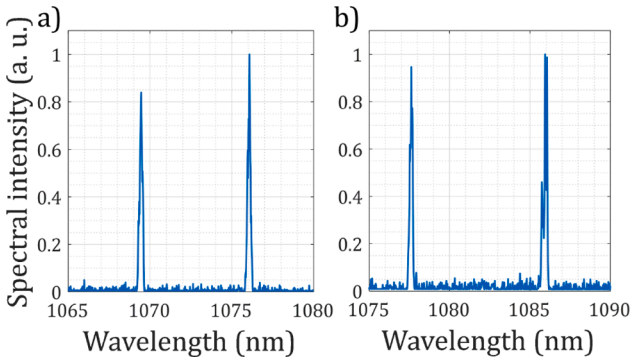

Fig. 7. Broad dual-wavelength oscillation at (a) 1069–1077 nm, and (b) 1077.5–1086.5 nm in Nd:KGW.

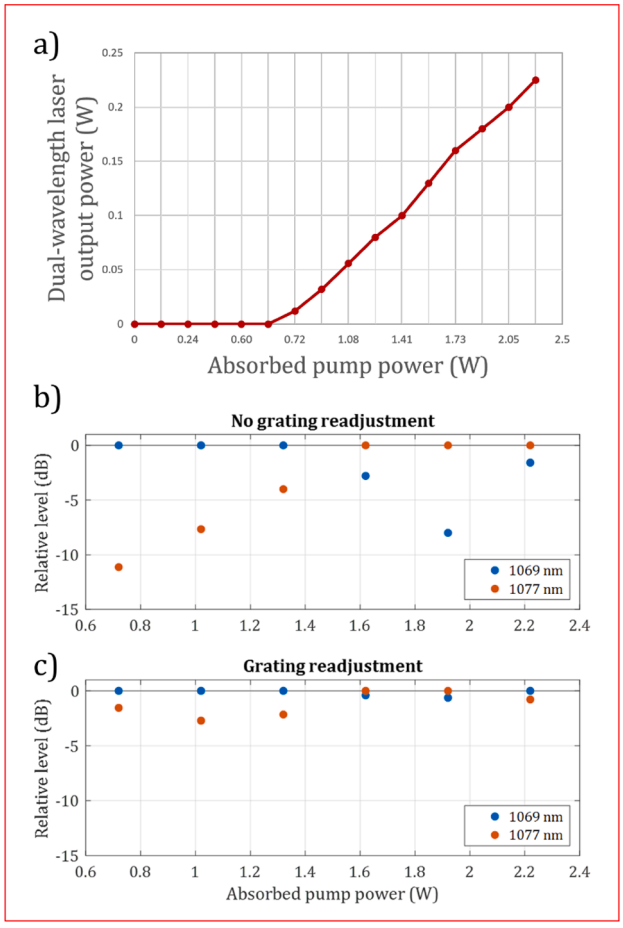

Fig. 8. (a) 1069–1077 nm dual-wavelength output power versus absorbed pump power. (b) Relative power between 1069 and 1077 nm for different absorbed pump powers, and (c) amplitude balancing with grating readjustment at each pump power.

the surrounding of 1067 nm, ~2 nm tuning at 1076 nm and ~1 nm tuning at 1085 nm.

We also assessed the thermal lens in our crystal in the configuration of Fig. 2. We registered the beam width evolution for the cavity M1-M2 in the range of 100 to 600 mm from M2 and adjusted it with ABCD matrices to the beam evolution for positive and negative lenses inside the M1-M2 cavity of different focal lengths [21]. The measured thermally induced dioptric power as a function of absorbed pump intensity is depicted in Fig. 6. As stated in [21], in N_p-cut Nd:KGW, the thermal is astigmatic and with opposite sign for N_m and N_g transverse planes. We

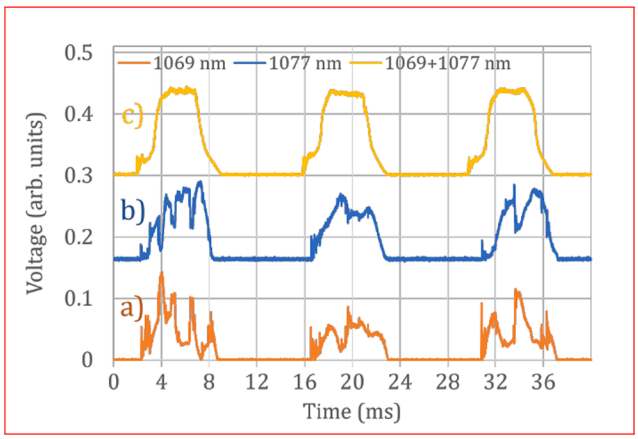

Fig. 9. Oscilloscope traces for short-term stability of a) 1069 nm, b) 1077 nm and c) 1069 + 1077 nm.

performed additional ABCD matrix calculations and found the external-cavity mode was stable for the measured span of thermal lenses but we also found that, with a single spherical lens (CL) in the external cavity, the external-cavity mode can not be matched to the main cavity mode in both N_m and N_g directions simultaneously. This means a penalty on the feedback efficiency when thermal lens is present and cannot be fully corrected with the actual external-cavity configuration. The sensitivity of effective feedback to thermal lens and to feedback spectral resolution will be object of further investigations in future research.

The laser can also be configured for dual-wavelength operation. Dual-wavelength operation in Nd:KGW has not been still reported either, to our knowledge. Dual-wavelength oscillation can be obtained with large wavelength-offset (i.e. ~1067–1076 nm or ~1076–1085 nm) or narrow wavelength-offset (i.e. oscillation of two wavelengths within the broadening of an emission cross-section spectral peak). For large wavelength-offset radiation, due to a non-perfectly smooth edge and pass bands, simultaneous oscillation at either 1067–1076 nm or 1076–1085 nm shows imbalanced thresholds, thus making it difficult dual-wavelength oscillation. The external-cavity grating can be used to balance the thresholds for dual-wavelength oscillation. In Fig. 7(a) dual-wavelength oscillation at 1069 and 1077 nm and in Fig. 7(b) oscillation at 1077.5 and 1086.5 nm are depicted. Regarding the stability of the dual-wavelength, we have studied the 1069–1077 nm oscillation as an example. The dual-wavelength 1069–1077 nm output power versus absorbed pump power is represented in Fig. 8(a) and resembles the 1076 nm output power curve in Fig. 5(a).

We have distinguished between long-term and short-term stability as the fluctuation seen in an OSA with few seconds averaging and the fluctuations in scales of few ms or shorter, respectively. For the long term stability we registered 1069 nm and 1077 nm amplitudes in an OSA with 5 s swept time at different pump powers. In Fig. 8(b) and 8(c), i.e., long-term stability, 0 dB represents the power of the wavelength with the highest amplitude and the lowest-amplitude wavelength power is then represented relative to 0 dB. In Fig. 8(b), the pump power is swept downwards from 2.2 W of absorbed power to 0.7 W. Although the dual-wavelength prevails the relative powers of the dual-wavelength spectral components are unbalanced in the range of 10 dB as the pump power is swept. In Fig. 8(c) data were recorded adjusting slightly the vertical tilt of the DF as the pump power was swept, yielding a nearly amplitude balanced dual-wavelength oscillation.

With respect to the short-term stability, the pump power was chopped at a frequency of 72 Hz. We spatially separated 1069 and 1077 nm power-balanced wavelengths and they were recorded simultaneously in two separate channels of an oscilloscope by two independent photodiodes (traces a) and b) in Fig. 9, respectively). Trace c) in Fig. 9, which was recorded later than a) and b), exhibits that the dual-wavelength

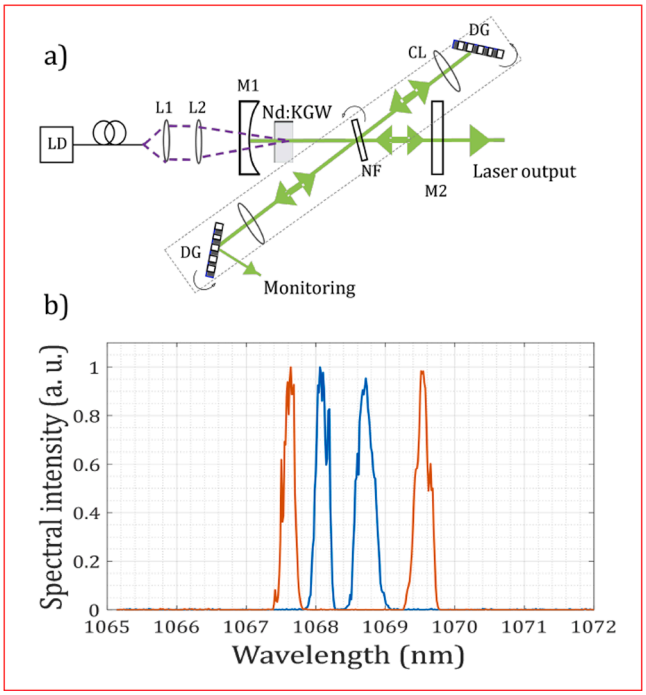

Fig. 10. (a) setup for narrow dual-wavelength oscillation. (b) Narrow dual-wavelength tuning within 1067 nm emission peak with spectral separation of 0.8 nm (blue line) and 2 nm (orange line).

oscillation, i.e. the sum of 1069 + 1077 nm, is stable in the short term although the separated wavelengths fluctuate competing for the shared gain. Small time-varying laser cavity perturbations may lead to an unbalanced dual-wavelength oscillation, i.e. if one wavelength increases its power, the other one reduces in the same amount. We believe fluctuations are the result of laser technical noise in our laboratory, mainly because of vibrations of chillers, fans and water flow through the laser crystal holder.

The insertion of an additional grating can also be adopted for either broad or narrow wavelength-offset. In particular, narrow-wavelength offset within the main emission peak is of interest in image upconversion applications [10,11]. The experimental setup for dual-wavelength operation with a narrow-wavelength offset is a modification of Fig. 3 (a) where an additional external cavity is included and M2 is changed to a reflectivity of 1%, acting as an output coupler (Fig. 10(a). In Fig. 10(b), two examples of narrow-wavelength tuning (0.8 nm and 2 nm) within the 1067 nm emission cross-section peak are shown. Nd:KGW is expected to provide a broader dual-wavelength offset over more widespread Nd-doped hosts such as YAG, YVO_4 or $GdVO_4$ where gain bandwidth is in the order of 0.6, 0.8 and 1.3 nm [23], respectively, in contrast to Nd:KGW with a 2.73 nm gain bandwidth [7].

4. Conclusion

To our knowledge, this work is a first investigation and experimental demonstration of wavelength selection and tuning in Nd:KGW. Our results leave still room for improvements in terms of efficiency and emission wavelength tuning range. We believe the asymmetric spatial distribution of the thermal dioptric power in N_p-cut crystal orientation, i.e. positive or negative sign for N_m and N_g crystal principal planes, respectively [21], avoids adequate mode matching of the main cavity and external-cavity feedback modes. Optimization of both the slope efficiency and the external-cavity feedback for tuning would then require a specifically designed setup for compensation of this kind of thermal lens including different optical elements for different transverse axes. Additionally, other crystal orientation lasing at either N_g or N_p polarization can be adopted to avoid the different sign of the dioptric power. Such crystal orientations also offer a broader emission spectrum, at the expense of lower absorption and emission cross-sections, which could potentially reach emission wavelengths from 1050 nm up to 1100 nm in the $^4F_{3/2}$ - $^4I_{11/2}$ transition. In addition, because of their better trade-off between spectral resolution and diffraction efficiency, volume Bragg gratings (VBGs) could replace the diffraction grating in the external cavity configuration for controlling the effective spectral shaping of the intracavity loss and improve laser performance in terms of operation mode (dual or single-wavelength) and tuning of the laser emission. Further investigations on external-cavity tuning in Nd:KGW are of interest for the development of monolithic Nd:KGW tunable self-Raman lasers. Our work can also be readily extended to the $^4F_{3/2}$ - $^4I_{9/2}$ and $^4F_{3/2}$ - $^4I_{13/2}$ transitions of the Nd^{3+} in KGW.

Declaration of Competing Interest

The authors declare that they have no known competing financial interests or personal relationships that could have appeared to influence the work reported in this paper.

Acknowledgement

This work was partially supported by Ministerio de Ciencia, Innovación y Universidades of Spain (TEC2017-88899-C2-1-R), Ministerio de Ciencia e Innovación of Spain (PID2020-117658RB-I00) and FEDER funds. All the authors contributed equally to this work.

References

[1] V.A. Berenberg, S.N. Karpukhin, I.V. Mochalov, Nonlinear optical effects and devices: Stimulated Raman scattering of nanosecond pulses in a $KGd(WO_4)_2$ crystal, Sov. J. Quantum Electron. 17 (1987) 1178–1179, https://doi.org/10.1070/QE1987v017n09ABEH009793.

[2] C.-Y. Tang, W.-Z. Zhuang, K.-W. Su, Y.-F. Chen, Efficient Continuous-Wave Self-Raman Nd:KGW Laser With Intracavity Cascade Emission Based on Shift of 89 cm^{-1}, IEEE J. Sel. Top. Quantum Electron. 21 (2015) 142–147, https://doi.org/10.1109/JSTQE.2014.2364126.

[3] P. Loiko, S. Yoon, J. Serres, X. Mateos, S. Beecher, R. Birch, V. Savitski, A. Kemp, K. Yumashev, U. Griebner, V. Petrov, M. Aguiló, F. Díaz, J. Mackenzie, Temperature-dependent spectroscopy and microchip laser operation of Nd:KGd $(WO_4)_2$, Opt. Mater. 58 (2016) 365–372, https://doi.org/10.1016/j.optmat.2016.06.005.

[4] K. Huang, W.Q. Ge, T.Z. Zhao, C.Y. Feng, J. Yu, J.G. He, H. Xiao, Z.W. Fan, High-power passively Q-switched Nd:KGW laser pumped at 877 nm, Appl. Phys. B 122 (6) (2016) 171, https://doi.org/10.1007/s00340-016-6439-3.

[5] R.C. Talukder, M. Halim, T. Waritanant, A. Major, Multiwatt continuous wave Nd:KGW laser with hot-band diode pumping, Opt. Lett. 41 (2016) 3810, https://doi.org/10.1364/OL.41.003810.

[6] T. Waritanant, A. Major, Diode-pumped Nd:YVO_4 laser with discrete multi-wavelength tunability and high efficiency, Opt. Lett. 42 (6) (2017) 1149–1152, https://doi.org/10.1364/OL.42.001149.

[7] Lasers - Optogama UAB [Online], https://4lasers.com/en/components/crystals/laser-crystals/nd-doped-crystals/nd-kgw-crystals (accessed 04-02-2022).

[8] R. Czarny, M. Alouini, C. Larat, M. Krakowski, D. Dolfi, THz-dual-frequency Yb^{3+}:$KGd(WO_4)_2$ laser for continuous wave THz generation through photomixing, Electron. Lett. 40 (2004) 942–943, https://doi.org/10.1049/el:20040597.

[9] A. Brenier, Two-frequency pulsed $YLiF_4$: Nd lasing out of the principal axes and THz generation, Opt. Lett. 40 (19) (2015) 4496–4499, https://doi.org/10.1364/OL.40.004496.

[10] H. Maestre, A.J. Torregrosa, J. Capmany, IR Image upconversion using band-limited ASE illumination fiber sources, Opt. Express 24 (8) (2016) 8581–8593, https://doi.org/10.1364/OE.24.008581.

[11] R. Demur, R. Garioud, A. Grisard, E. Lallier, L. Leviandier, L. Morvan, N. Treps, C. Fabre, Near-infrared to visible upconversion imaging using a broadband pump laser, Opt. Express 26 (10) (2018) 13252–13263, https://doi.org/10.1364/OE.26.013252.

[12] M. Funayama, K. Mukaihara, H. Morita, T. Okada, N. Tomonaga, J. Izumi, Y. Noda, M. Maeda, Widely Tunable Operation of Ti: Sapphire Lasers under Optimum Coupling Condition, Jpn. J. Appl. Phys. 32 (Part 2, No. 9B) (1993) L1332–L1334, https://doi.org/10.1143/jjap.32.l1332.

[13] Q. Sheng, A. Lee, D. Spence, H. Pask, Wavelength tuning and power enhancement of an intracavity Nd:$GdVO_4$-$BaWO_4$ Raman laser using an etalon, Opt. Express 26 (24) (2018) 32145–32155, https://doi.org/10.1364/OE.26.032145.

[14] M. Tsunekane, M. Ihara, N. Taguchi, H. Inaba, Analysis and design of widely tunable diode-pumped Cr:LiSAF lasers with external grating feedback, IEEE J. Quantum Electron. 34 (1998) 1288–1296, https://doi.org/10.1109/3.687874.
[15] Q. Sheng, R. Li, A.J. Lee, D.J. Spence, H.M. Pask, A single-frequency intracavity Raman laser, Opt. Express 27 (6) (2019) 8540–8553, https://doi.org/10.1364/OE.27.008540.
[16] M.T. Chang, H.C. Liang, K.W. Su, Y.F. Chen, Dual-comb self-mode-locked monolithic Yb:KGW laser with orthogonal polarizations, Opt. Express 23 (8) (2015) 10111–10116, https://doi.org/10.1364/OE.23.010111.
[17] X. Qiao, P. Sun, X. Wang, H. Wang, J. Dong, Broadband multi-longitudinal-mode Yb:YAG/YVO_4 coupled Raman microchip laser, J. Phys. Photonics 2 (4) (2020) 045007, https://doi.org/10.1088/2515-7647/abac1b.
[18] U. Demirbas, R. Uecker, J.G. Fujimoto, A. Leitenstorfer, Multicolor lasers using birefringent filters: experimental demonstration with Cr:Nd:GSGG and Cr:LiSAF, Opt. Express 25 (3) (2017) 2594–2607, https://doi.org/10.1364/OE.25.002594.
[19] T. Graf, J.E. Balmer, Lasing Properties of Diode Laser-Pumped Nd:KGW, in: Advanced Solid State Lasers, Optical Society of America, 1995, p. LM5. https://doi.org/10.1364/ASSL.1995.LM5.
[20] Y. Kalisky, L. Kravchik, C. Labbe, Repetitive modulation and passively Q-switching of diode-pumped Nd-KGW laser, Opt. Commun. 189 (1) (2001) 113–125, https://doi.org/10.1016/S0030-4018(01)01018-5.
[21] P. Loiko, K. Yumashev, N. Kuleshov, V. Savitski, S. Calvez, D. Burns, A. Pavlyuk, Thermal lens study in diode pumped Ng- and Np-cut Nd:$KGd(WO_4)_2$ laser crystals, Opt. Express 17 (26) (2009) 23536–23543, https://doi.org/10.1364/OE.17.023536.
[22] H. Maestre, A.J. Torregrosa, J.A. Pereda, C.R. Fernández-Pousa, J. Capmany, Dual-Wavelength Cr^{3+} : $LiCaAlF_6$ Solid-State Laser With Tunable THz Frequency Difference, IEEE J. Quantum Electron. 46 (11) (2010) 1681–1685, https://doi.org/10.1109/JQE.2010.2058999.
[23] S. Ng, D. Tang, J. Kong, Z. Xiong, T. Chen, L. Qin, X. Meng, Quasi-cw diode-pumped Nd:$GdVO_4$ laser passively Q-switched and mode-locked by Cr^{4+}:YAG saturable absorber, Opt. Commun. 250 (1) (2005) 168–173, https://doi.org/10.1016/j.optcom.2005.02.018.